

2017-09

# In situ determination of trace elements in *Fucus* spp. by field-portable-XRF

Turner, Andrew

<http://hdl.handle.net/10026.1/8819>

---

10.1016/j.scitotenv.2017.03.091

Science of The Total Environment

Elsevier BV

---

*All content in PEARL is protected by copyright law. Author manuscripts are made available in accordance with publisher policies. Please cite only the published version using the details provided on the item record or document. In the absence of an open licence (e.g. Creative Commons), permissions for further reuse of content should be sought from the publisher or author.*

1  
2  
3 **In situ determination of trace elements in *Fucus* spp. by**  
4 **field-portable-XRF**  
5

6  
7 **Andrew Turner\*, Hiu Poon, Alex Taylor & Murray T. Brown<sup>1</sup>**

8  
9 *School of Geography, Earth and Environmental Sciences and <sup>1</sup>School of Biological and*  
10 *Marine Sciences, Plymouth University, Drake Circus, Plymouth PL4 8AA, UK*  
11

12  
13  
14 \*Corresponding author. Tel: +44 1752 584570; Fax: +44 1752 584710; e-mail:  
15 [aturner@plymouth.ac.uk](mailto:aturner@plymouth.ac.uk)  
16

17  
18 Accepted 9 March 2017

19 <http://dx.doi.org/10.1016/j.scitotenv.2017.03.091>

20 Embargo period 1/9/2019  
21  
22  
23

24 **Abstract**

25 Fresh and freeze-dried sample sections of the coastal macroalgae, *Fucus serratus* and *F.*  
26 *vesiculosus*, and the brackish water macroalga, *F. ceranoides*, have been analysed for trace  
27 elements by field-portable-x-ray fluorescence (FP-XRF) spectrometry using a Niton XL3t in  
28 a low density mode with thickness correction. When analysed fresh in a laboratory accessory  
29 stand for a period of 200 seconds, As, Br, Fe and Zn were registered in the apex, mid-frond  
30 and lower stipe of all species, with detection limits of a few  $\mu\text{g g}^{-1}$  (As) or a few tens of  $\mu\text{g g}^{-1}$   
31 (Br, Fe, Zn); when analysed dry under the same conditions, concentrations returned were  
32 systematically higher and Cu and Pb were detected in a number of *F. ceranoides* sections.  
33 Concentrations arising from both approaches on a dry weight basis were highly correlated,  
34 with deviations from unit slope attributed to the absorption of fluorescent x-rays by internal  
35 and surficial water when analysed fresh. With algorithms correcting for the effects of water  
36 on mass and x-ray absorption, sections of *F. vesiculosus* and *F. ceranoides* were analysed in  
37 situ with the XRF connected to a mobile stand and laptop. Dry weight concentrations  
38 returned for As and Zn were significantly correlated with respective concentrations  
39 subsequently determined by ICP-MS following acid digestion and with a slope close to  
40 unity; lower concentrations of Fe returned by ICP were attributed to the incomplete acid  
41 digestion of silt particles that evaded an initial cleaning step, while Br concentrations could  
42 not be verified independently because of loss of volatile forms during digestion. The in situ  
43 determination of trace elements in fucoids by FP-XRF provides a rapid and non-destructive  
44 means of monitoring environmental quality and identifying hot-spots of contamination, and  
45 enables a research strategy to be developed iteratively that is informed by immediate results.

46

47 **Keywords:** macroalgae; fucoids; FP-XRF; monitoring; trace elements; ICP-MS

48 **1. Introduction**

49 Marine macroalgae represent a large and diverse group of primary-producing organisms in  
50 the coastal zone that create habitat structure, provide food, promote biodiversity and serve as  
51 a carbon sink (Duarte et al., 2013; Matias et al., 2015). Macroalgae also have an economic  
52 value, acting as a source of food, nutrients and medicines for human consumption and  
53 offering a means of bioremediation and a potential bioenergy resource (Bruhn et al., 2011;  
54 Tabarsa et al., 2012). Being sessile, macroalgae are influenced directly by ambient  
55 environmental conditions, and in this respect the distribution and occurrence of certain  
56 species may often reflect local water quality (Guinda et al., 2008). Moreover, because of  
57 their thick cell walls and high polysaccharide content, macroalgae are also able to  
58 accumulate many aqueous contaminants, and in particular trace metals and metalloids, to  
59 concentrations several thousand times higher than the ambient water column (Zbikowski et  
60 al., 2006). Consequently, many species act as vehicles for the transfer of contaminants up the  
61 food chain (Chan et al., 2003; Mulholland and Turner, 2011) and serve as useful biomonitors  
62 that provide a direct and integrated assessment of bioavailable contaminants over a period of  
63 time (Cairrão et al., 2007; Boubonari et al., 2008). The littoral brown fucoids are particularly  
64 useful in the latter respect because of their extensive distribution, ease of identification and  
65 sampling, tolerance of wide variations of temperature and salinity, abundance all year round  
66 and limited ability to regulate contaminant concentrations (Martin et al., 1997; Rainbow,  
67 2006; Sondergaard et al., 2014). Accordingly, *Fucus* spp. have been selected for inclusion in  
68 the Environmental Specimen Banks (ECBs) of several European countries in order to  
69 monitor long-term changes in anthropogenic contamination (Viana et al., 2010; Rüdél et al.,  
70 2010).

71

72 As commonly employed biomonitor organisms, there is a requirement for the routine  
73 determination of trace elements in macroalgae. Conventionally, analysis is performed on

74 dried samples that have been digested in hot, concentrated acid by, for example, atomic  
75 absorption spectrometry (Reis et al., 2014) or inductively coupled plasma (ICP)  
76 spectrometry (Brito et al., 2012). This approach can, however, be time-consuming, labour-  
77 intensive and costly, and the destruction of samples has implications for the long-term  
78 viability of archived specimen banks. Recently, we investigated the feasibility of field  
79 portable-x-ray fluorescence (FP-XRF) spectrometry as a rapid, non-destructive means of  
80 determining trace elements in various species of macroalgae (Bull et al., 2017). Specifically,  
81 we employed a Niton XL3t spectrometer configured in a low density, ‘plastics’ mode and  
82 with a corrective algorithm for sample thickness to measure dried samples housed in a  
83 laboratory accessory stand. For the elements that were detected, there was a significant  
84 correlation between concentrations measured directly and those returned independently by  
85 ICP-mass spectrometry following HNO<sub>3</sub> digestion, with relationships satisfying the EPA  
86 definitive level criterion for As and quantitative screening level for Cu and Zn  
87 (Environmental Protection Agency, 2007).

88

89 In order to further the XRF approach for measurements of trace elements in macroalgae in  
90 situ, the effects of water, as a contributor to both sample mass and x-ray absorption, need to  
91 be accounted for and factored in to any calibration. To this end, the present study compares  
92 trace element concentrations returned by FP-XRF for different species of macroalgae  
93 analysed both in the fresh and freeze-dried states. Specifically, fucoids were selected because  
94 of their importance in coastal biomonitoring and their relatively high thickness (for x-ray  
95 absorption) compared with other species of macroalgae (Bull et al., 2017). With the effects  
96 of water empirically quantified, the practicalities and challenges of deploying the XRF in the  
97 field for the direct measurement of trace elements in macroalgae are discussed.

98

99

100

101 **2. Materials and methods**

102 *2.1. Sampling and sample preparation*

103 Whole samples of furoid were handpicked at low tide in July 2016 from two sites within 25  
104 minutes' driving distance of the laboratory at Plymouth University (Figure 1). At Firestone  
105 Bay, a small, pebble-sand beach in the coastal embayment of Plymouth Sound, five  
106 specimens of two coastal furoids, *F. serratus* and *F. vesiculosus*, were collected from the  
107 rocky substrates of the littoral zone and stored in a cool box in a series of zip-lock  
108 polyethylene bags. From the intertidal mudflats of the upper Tavy Estuary, a tidal tributary  
109 of the Tamar Estuary and an environment impacted by historical mining activities, ten  
110 specimens of *F. ceranoides*, a brackish water furoid, were collected and stored likewise. In  
111 the laboratory, samples of *F. serratus* and *F. vesiculosus* were divided and subjected to two  
112 different methods of clearing sediment and epiphytes from the surface; thus, one half was  
113 cleaned in Millipore Milli-Q water (MQW) with the aid of a Nylon brush and subsequently  
114 scraped with a plastic spatula after applying a 10% solution of ethanol to the tissue surface,  
115 while the other half was cleaned with MQW only. After blotting dry with 3-ply hygiene roll,  
116 all plants were dissected on a plastic tray using a stainless steel blade, with ~ 5 cm sections  
117 of the apex, mid-frond and lower stipe (just above the holdfast) from each plant retained and  
118 stored in individual specimen bags. Because of the smaller size of *F. ceranoides* and results  
119 arising from the cleaning methods of the two coastal macroalgae, samples of the brackish  
120 water furoid were cleaned in MQW only before being dissected likewise.

121

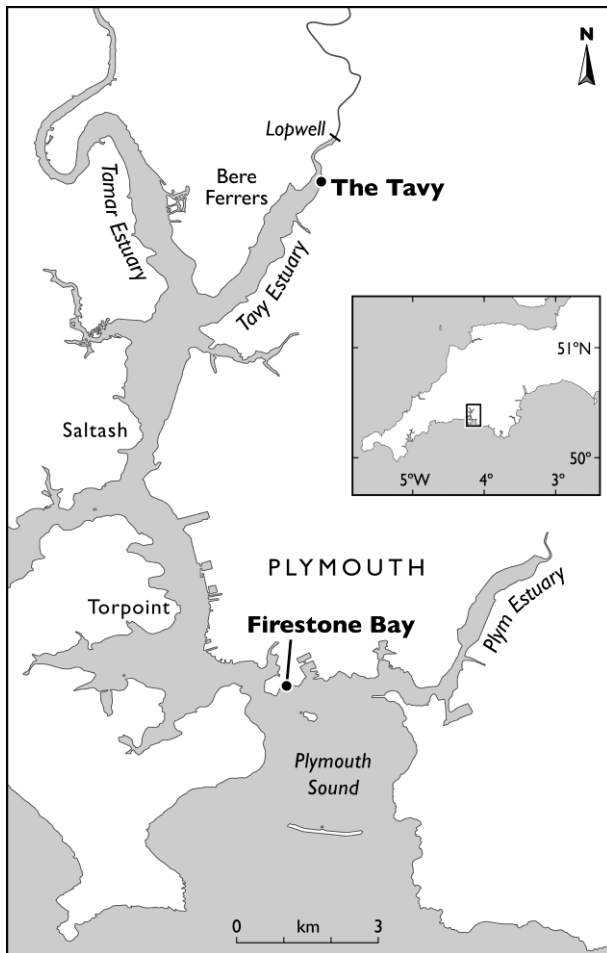
122

123

124

125

126



127

128 Figure 1: The sampling locations for the fucoid macroalgae.

129

130 *2.2. FP-XRF analysis*

131 Sample sections processed in the laboratory ( $n = 90$ ) were analysed for trace elements (As,  
 132 Br, Cd, Cr, Cu, Fe, Hg, Ni, Pb and Zn) directly and without drying by energy dispersive FP-  
 133 XRF using a battery-powered, 1.3 kg Niton analyser (model XL3t 950 He GOLDD+) housed  
 134 in a ThermoScientific accessory stand of steel construction and tungsten-plastic shielding  
 135 (PN 420-017; weight  $\sim 10$  kg, chamber volume =  $4000 \text{ cm}^3$ ). Analysis was performed in a  
 136 low density mode that uses a fundamental parameters-based alpha coefficient correction  
 137 model (Turner and Solman, 2016). Because the intensity of fluorescence generated by low  
 138 density and weakly absorbing samples is dependent on the thickness of material, a corrective  
 139 algorithm (down to  $50 \mu\text{m}$ ) was also applied after section thickness had been measured in  
 140 mm and to two decimal places using digital callipers. With plastic tweezers, samples were

141 placed onto a SpectraCertified Mylar polyester 3.6  $\mu\text{m}$  film, which was then positioned  
142 carefully such that the smoothest and flattest part of the macroalgal section lay directly and  
143 centrally above the 8 mm XRF detector window. After closing the accessory stand lid, the  
144 XRF was activated remotely and via USB using a Fujitsu laptop computer. Analysis was  
145 tested for a variety of conditions of which a collimation of 8 mm and a counting period of  
146 200 seconds, comprising 150 seconds at 50 kV and 40  $\mu\text{A}$  and 50 seconds at 20 kV and 100  
147  $\mu\text{A}$ , appeared to be optimal in terms of detection, error and sample throughput. To check the  
148 performance of the XRF and as an analytical quality control, Niton polyethylene reference  
149 discs impregnated with known concentrations of various trace elements (PN 180-619,  
150 LOT#T-18 and PN 180-554, batch SN PE-071-N) were analysed throughout each  
151 measurement session. On completion of measurements, spectra and elemental concentrations  
152 (in  $\mu\text{g g}^{-1}$  and with a counting error of  $2\sigma$ ) were downloaded to the laptop using Niton Data  
153 Transfer PC software.

154

155 Immediately after sample measurement, individual macroalgal sections were weighed using  
156 a five-figure Sartorius analytical balance before being returned to their original specimen  
157 bags and freeze-dried for 48 h using an Edwards Super Modulyo. Dried sections were then  
158 re-analysed by XRF under the operating conditions described above and after appropriate  
159 (dry) thickness correction, before being re-weighed, returned to their specimen bags and  
160 stored under desiccation pending acid digestion (see below).

161

### 162 *2.3. Macroalgae digestion and analysis by ICP-MS*

163 As an independent measure of trace elements in the macroalgae, all freeze-dried sample  
164 sections were subsequently acid-digested and analysed by inductively coupled plasma-mass  
165 spectrometry (ICP-MS). Thus, samples of about 0.1 g were accurately weighed into  
166 individual Teflon tubes to which 2.5 ml aliquots of  $\text{HNO}_3$  (Fisher Chemical TraceMetal™



167 Grade) were added. The contents were digested in a CEM MARS 5 XPRESS microwave at  
168 1600 W for 45 min before being allowed to cool to room temperature. Digests were then  
169 washed into individual 10 ml volumetric flasks and diluted to mark with ultra-pure Millipore  
170 Milli-Q water. For an assessment of digestion efficacy and analytical accuracy, a fucoid  
171 reference material (*Fucus vesiculosus*, ERM-CD200; certified for As, Br, Cd, Cu, Fe, Hg,  
172 Pb, Se and Zn) was digested in triplicate likewise.

173

174 Digests were analysed for elements that had been detected by XRF using a collision cell-  
175 ICP-MS (Thermo X-series II, Thermoelemental, Winsford, UK) with a concentric glass  
176 nebuliser and conical spray chamber. RF power was set at 1400 W and coolant, auxiliary,  
177 nebuliser and collision cell gas flows rates were 13 L Ar min<sup>-1</sup>, 0.70 L Ar min<sup>-1</sup>, 0.72 L Ar  
178 min<sup>-1</sup> and 3.5 mL 7% H<sub>2</sub> in He min<sup>-1</sup>, respectively. The instrument was calibrated externally  
179 using four mixed standards prepared by dilutions of a QC 26 multi-element solution (CPI  
180 International, Amsterdam) in 0.1 M HNO<sub>3</sub>, and internally by the addition of 100 µg L<sup>-1</sup> of In  
181 and Ir to all samples and standards. Data were acquired over a dwell period of 10 ms, with  
182 50 sweeps per reading and three replicates.

183

184 Aqueous concentrations derived from ICP-MS were converted to dry weight concentrations  
185 (in µg g<sup>-1</sup>) from the volume of diluted digest and mass of macroalga dissolved in acid. Limits  
186 of detection on this basis were < 2.5 µg g<sup>-1</sup> for all trace elements analysed, and measured  
187 concentrations in the reference macroalga were within 15% of published values with the  
188 exception of Br and Fe (recoveries of about 50% and 70%, respectively).

189

#### 190 2.4. Statistical analysis

191 Correlation analysis was performed on paired data series using the Data Analysis Toolpak in  
192 Excel 2016, with the strength of association reported as Pearson's moment correlation

193 coefficient ( $r$ ) and the significance of the relationship as the probability of  $r$  not being  
194 different from zero ( $p$ , and where  $\alpha = 0.05$ ). One-way ANOVA and Tukey's post-hoc test  
195 were used in Minitab 17 to identify significant differences ( $\alpha = 0.05$ ) in mean elemental  
196 concentrations and water contents among macroalgae and parts thereof, and in mean  
197 elemental concentrations arising from the three analytical methods.

198

### 199 **3. Results and Discussion**

#### 200 *3.1. Macroalgal water content and thickness*

201 Quantification of the water content of the macroalgal sections is critical for converting  
202 elemental concentrations from a fresh weight basis to a dry weight basis and for evaluating  
203 the impact of the fluid on x-ray behaviour and intensity (mainly through photoelectric  
204 absorption, but also via Compton scattering and internal reflections; Parsons et al., 2013).  
205 Mean percentage water, calculated from the fresh and dry weights of each section and shown  
206 in Table 1, ranged from about 50% to nearly 90%, and for all species the order of descending  
207 water content was: apex > mid-frond > lower stipe. There was no statistical difference in  
208 water content between common sections of *F. vesiculosus* and *F. serratus*, but the water  
209 content of sections of *F. ceranoides* were significantly greater than corresponding sections of  
210 the former two species. The method of tissue cleaning made a difference to mean water  
211 content that was significant only for the lower-stipe of *F. vesiculosus* from Firestone Bay.  
212 Thus, here, cleaning in MQW resulted in a higher percentage compared with sections having  
213 undergone additional cleaning with ethanol  
214  
215 Furoid section thickness, measured for XRF data correction, did not display a clear  
216 dependency on species, location with respect to the frond or means of tissue cleaning. On  
217 average, however, sections were thicker while wet ( $1.02 \pm 0.15$  mm) than when freeze-dried  
218 ( $0.85 \pm 0.19$  mm).

219

220 Table 1: Percentage water content of the fucoid macroalgal sections undergoing cleaning in  
221 Milli-Q water (MQW) and ethanol, and/or MQW only. The mean and standard deviation of  
222  $n$  measurements is given in each case.

	<i>F. serratus</i> (n=5)		<i>F. vesiculosus</i> (n=5)		<i>F. ceranoides</i> (n=10)
	MQW	MQW+ethanol	MQW	MQW+ethanol	MQW
apex	81.2 $\pm$ 1.8	76.3 $\pm$ 2.4	77.7 $\pm$ 2.2	73.1 $\pm$ 1.7	86.7 $\pm$ 1.9
mid-frond	67.7 $\pm$ 4.0	63.7 $\pm$ 5.1	62.6 $\pm$ 3.7	60.3 $\pm$ 2.8	76.9 $\pm$ 4.8
lower stipe	61.1 $\pm$ 1.7	54.2 $\pm$ 5.3	61.8 $\pm$ 1.3	51.8 $\pm$ 2.1	70.5 $\pm$ 3.6

223

### 224 3.2. XRF detection limits for trace elements in macroalgae

225 XRF detection limits for trace elements in the fucoids, defined as three counting errors for a  
226 200-second counting time, are presented in Table 2. Here, limits for all species, sectional  
227 locations and cleaning methods have been pooled and are shown for samples analysed in  
228 both the fresh state and after freeze-drying; with regard to the former, limits are shown on a  
229 fresh weight basis and, after correction for water content, a dry weight basis. Note that for  
230 some elements (Cd, Cr, Cu, Hg, Ni, Pb) limits have been averaged from at least fifteen  
231 measurements in which the element was not detected by the instrument but a value of  $3\sigma$   
232 was returned directly; where less than fifteen sample sections were undetectable (As, Br, Fe,  
233 Zn), limits were based on the values of  $2\sigma$  returned on detection and after multiplication by  
234 1.5.

235

236 Mean detection limits are generally lower when samples are analysed fresh than when  
237 freeze-dried, presumably because the greater flexibility of wet macroalgal sections allows  
238 them to be placed closer to the detector window of the instrument. However, when wet  
239 weight concentrations are converted to a dry weight basis, detection limits are higher than  
240 samples analysed dry. Here, we surmise that the effects of water on elemental dilution and x-

241 ray absorption and scattering outweigh the benefits of increased proximity to the detector.  
 242 Overall, mean detection limits are lowest and average less than  $10 \mu\text{g g}^{-1}$  (on both a dry  
 243 weight and wet weight basis) for As and Pb and are less than  $25 \mu\text{g g}^{-1}$  for Br, Cu, Hg, Ni  
 244 and Zn, and are similar to corresponding limits reported for dried sections of *F. serratus*  
 245 reported by Bull et al. (2017). Within these constraints, As and Fe were detected in all fucoid  
 246 section analyses performed in the present study ( $n = 180$ ), while Br and Zn were detected in  
 247 178 and 172 cases, respectively, with non-detection always associated with the analysis of  
 248 fresh samples. Note that although Cu and Pb were detected in some samples of *F.*  
 249 *ceranoides*, the number of cases ( $n = 7$  and  $n = 5$ , respectively) was too few for establishing  
 250 relationships between the different analytical approaches and differences among the three  
 251 sectional components of the macroalga.

252

253 Table 2: A summary (as mean  $\pm$  one standard deviation;  $n > 15$ ) of the Niton XRF detection  
 254 limits for trace elements in fucoid macroalgae analysed fresh and dry and for a 200-second  
 255 counting time (dw = dry weight; fw = fresh weight).

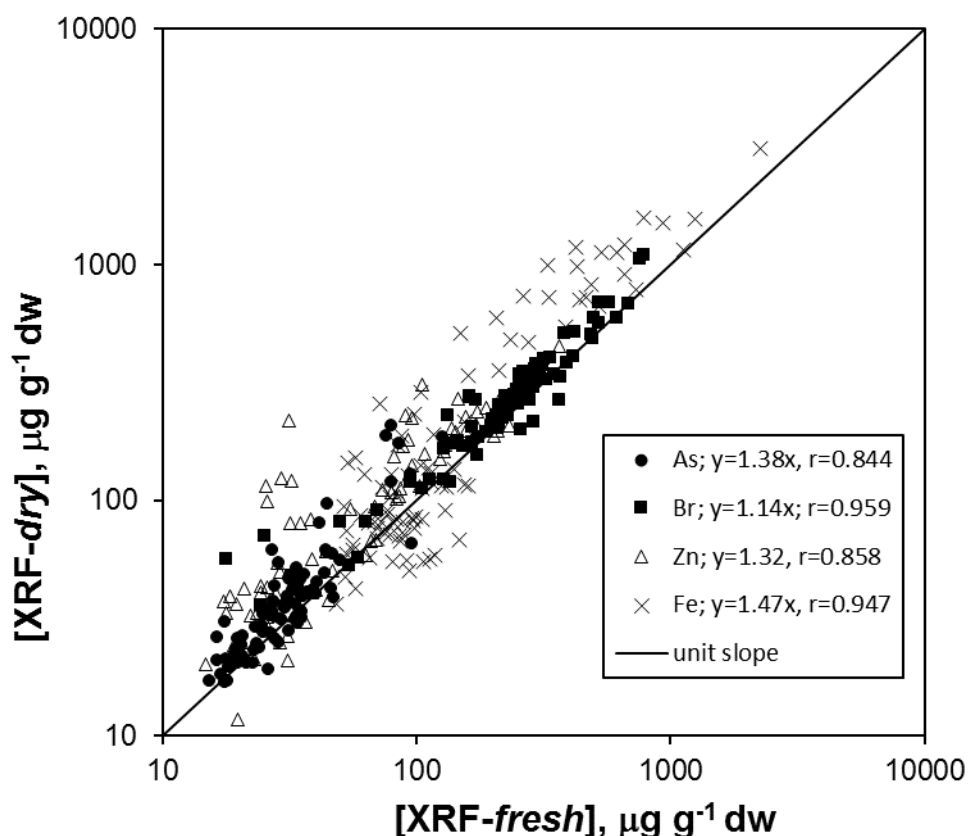
	As	Br	Cd	Cr	Cu	Fe	Hg	Ni	Pb	Zn
dry, $\mu\text{g g}^{-1}$ dw	4.7 $\pm$ 1.0	17.9 $\pm$ 4.6	26.3 $\pm$ 2.3	6.1 $\pm$ 2.2	16.2 $\pm$ 4.2	24.5 $\pm$ 6.7	12.3 $\pm$ 2.8	14.4 $\pm$ 3.8	5.9 $\pm$ 1.0	11.7 $\pm$ 2.7
fresh, $\mu\text{g g}^{-1}$ fw	1.6 $\pm$ 0.2	4.7 $\pm$ 1.2	14.4 $\pm$ 2.4	7.9 $\pm$ 2.0	5.3 $\pm$ 1.0	6.8 $\pm$ 1.3	5.0 $\pm$ 1.2	5.0 $\pm$ 1.0	2.3 $\pm$ 0.5	3.5 $\pm$ 1.1
256 fresh, $\mu\text{g g}^{-1}$ dw	6.6 $\pm$ 2.0	20.1 $\pm$ 9.5	61.0 $\pm$ 23.4	32.3 $\pm$ 11.9	22.2 $\pm$ 8.5	28.2 $\pm$ 10.1	21.2 $\pm$ 9.0	21.0 $\pm$ 8.9	9.7 $\pm$ 3.8	14.3 $\pm$ 5.5

257

### 258 3.3. Comparison of elemental concentrations when analysed wet and dry

259 Figure 2 compares the dry weight concentrations of readily detectable elements (As, Br, Fe,  
 260 Zn) in the fucoids that were returned by the Niton XRF when analysed dry, [XRF-dry], and  
 261 when analysed fresh and individually corrected for water content, [XRF-fresh]. Note that  
 262 here, data for each element are not discriminated by species, location on the frond or means  
 263 of tissue cleaning. Also shown are the best-fit equations (forced through the origin) that  
 264 define each element, along with corresponding Pearson's moment correlation coefficients

265 and the line signifying unit slope. In all cases, and despite changes in thickness and  
 266 morphology incurred by freeze-drying, elemental concentrations arising from both  
 267 approaches were highly correlated ( $p < 0.01$ ) with gradients exceeding unit value; that is,  
 268 concentrations returned when analysed dry were, on average, higher than concentrations  
 269 returned when analysed fresh but dry-weight corrected. This suggests that the presence of  
 270 internal and surficial water suppresses the strength of fluorescent x-rays reaching the  
 271 detector window of the FP-XRF through absorption and scattering. Consistent with this  
 272 assertion, deviation from unit slope is greatest for Fe, whose characteristic x-rays are of low  
 273 energy ( $K_{\alpha} = 6.405$  keV;  $L_{\alpha} = 0.705$  keV) and relatively easily absorbed by water, and least  
 274 for Br, whose characteristic x-rays are of higher energy ( $K_{\alpha} = 11.924$  keV;  $L_{\alpha} = 1.481$  keV)  
 275 and, therefore, less easily absorbed.



276  
 277 Figure 2: Dry weight elemental concentrations in the coastal and brackish water fucoid  
 278 macroalgae returned by the Niton XRF when analysed dry and fresh. Shown inset for each  
 279 element are equations of best fit when forced through the origin.

280

281 3.4. Inter- and intra-species variations in elemental concentrations and comparison with

282 ICP-MS

283 Figures 3 to 6 show the dry-weight concentrations of As, Br, Fe and Zn in the different parts

284 of each species of furoid and as determined by the two XRF approaches (that is, analysis of

285 fresh sections versus analysis of freeze-dried sections) and by ICP-MS following acid

286 digestion. Note that all data presented are for tissues cleaned in MQW only and that results

287 arising from samples subjected to additional cleaning with ethanol were very similar.

288 Regarding As, mean concentrations were not statistically different among the different

289 methods of determination with the exception of the lower stipe in *F. serratus*, where

290 concentrations were lower when analysed by XRF in the fresh state than by ICP, and the

291 apex in *F. ceranoides*, where concentrations were higher when analysed dry by XRF.

292 Among the different parts of the frond, mean concentrations were generally higher in the

293 apex than the mid-frond and lower stipe, an effect that was evident from each analytical

294 approach in at least one species of furoid. Overall, absolute concentrations of As were

295 greatest in the apex of *F. ceranoides*, and concentrations were significantly greater in the

296 mid-frond and lower stipe of *F. ceranoides* than in corresponding parts of both *F. serratus*

297 and *F. vesiculosus* according to at least one analytical approach.

298

299 With respect to Br, results arising from ICP-MS analysis have been neglected due to loss of

300 volatile forms (e.g. HBr and Br<sub>2</sub>) during acid-oxidizing digestion, an effect that is often

301 significant when opening the digestion vessel at the end of the mineralisation process (Di

302 Narda et al., 2001). Mean concentrations of the halogen were never statistically different

303 between the two XRF approaches and concentrations were not different among the three

304 sectional components of *F. serratus*. Concentrations were, however, significantly lower in

305 the stipe of *F. vesiculosus* than in its apex, and significantly higher in the stipe of *F.*  
306 *ceranoides* than in the apex where the lowest overall mean concentrations were observed.

307

308 Among the elements readily detected, concentrations of Fe were most variable among  
309 replicates. Consequently, there were no statistical differences observed between the two  
310 XRF approaches, despite mean concentrations returned being double when analysed dry in  
311 some cases. Determination by ICP-MS returned significantly lower concentrations than one  
312 or both XRF approaches (and by factors up to an order of magnitude) for the mid-fronds of  
313 both *F. serratus* and *F. ceranoides* and the apex and lower stipe of the latter.

314

315 Statistical differences in the mean concentrations of Zn were observed among the three  
316 analytical approaches only for the lower stipe of *F. vesiculosus* (lower by XRF after section  
317 drying), and the apex of *F. serratus* and apex and mid-frond of *F. ceranoides* (higher when  
318 analysed by XRF after drying than by both other approaches). With the exception of the apex  
319 analysed by XRF when fresh, mean concentrations of Zn were always statistically higher in  
320 *F. ceranoides* than corresponding concentrations in *F. vesiculosus*. In fewer cases, mean  
321 concentrations were higher in *F. ceranoides* than in *F. serratus* and in *F. serratus* than in *F.*  
322 *vesiculosus*.

323

324

325

326

327

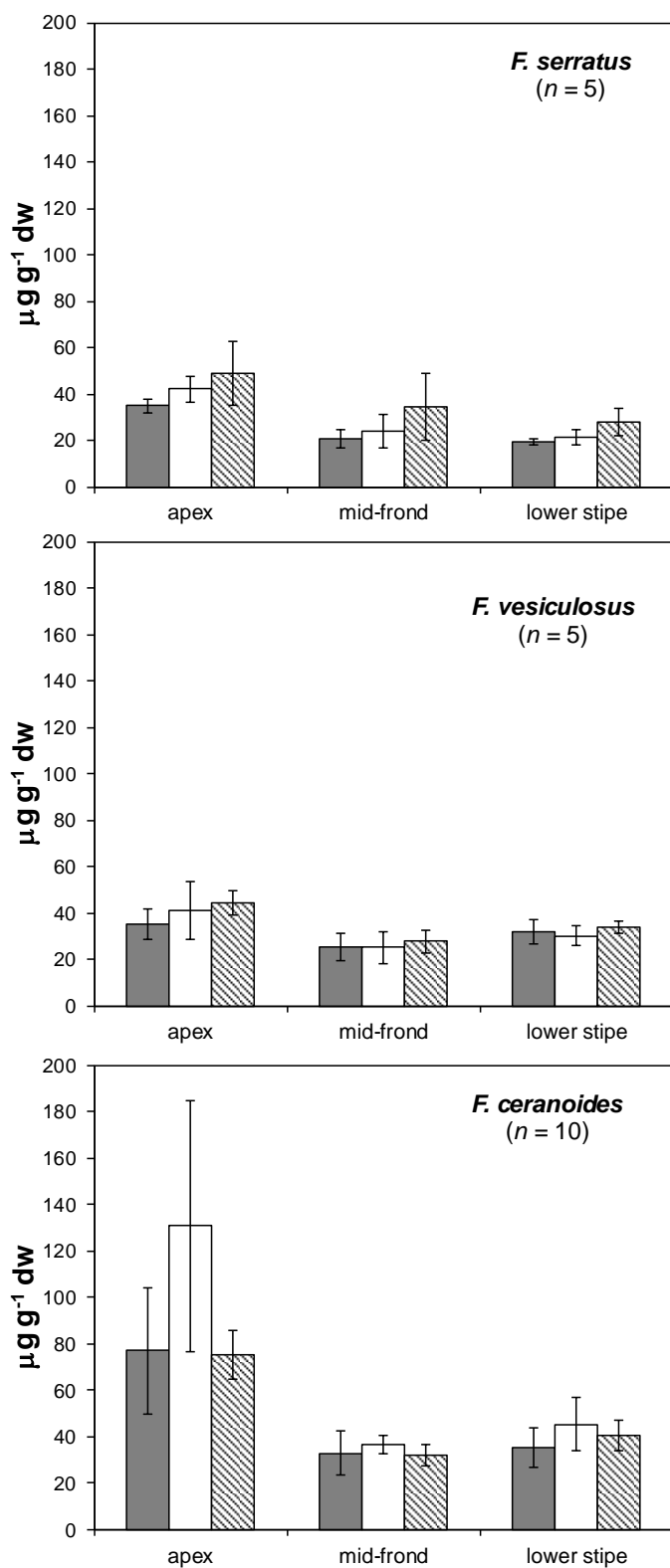
328

329

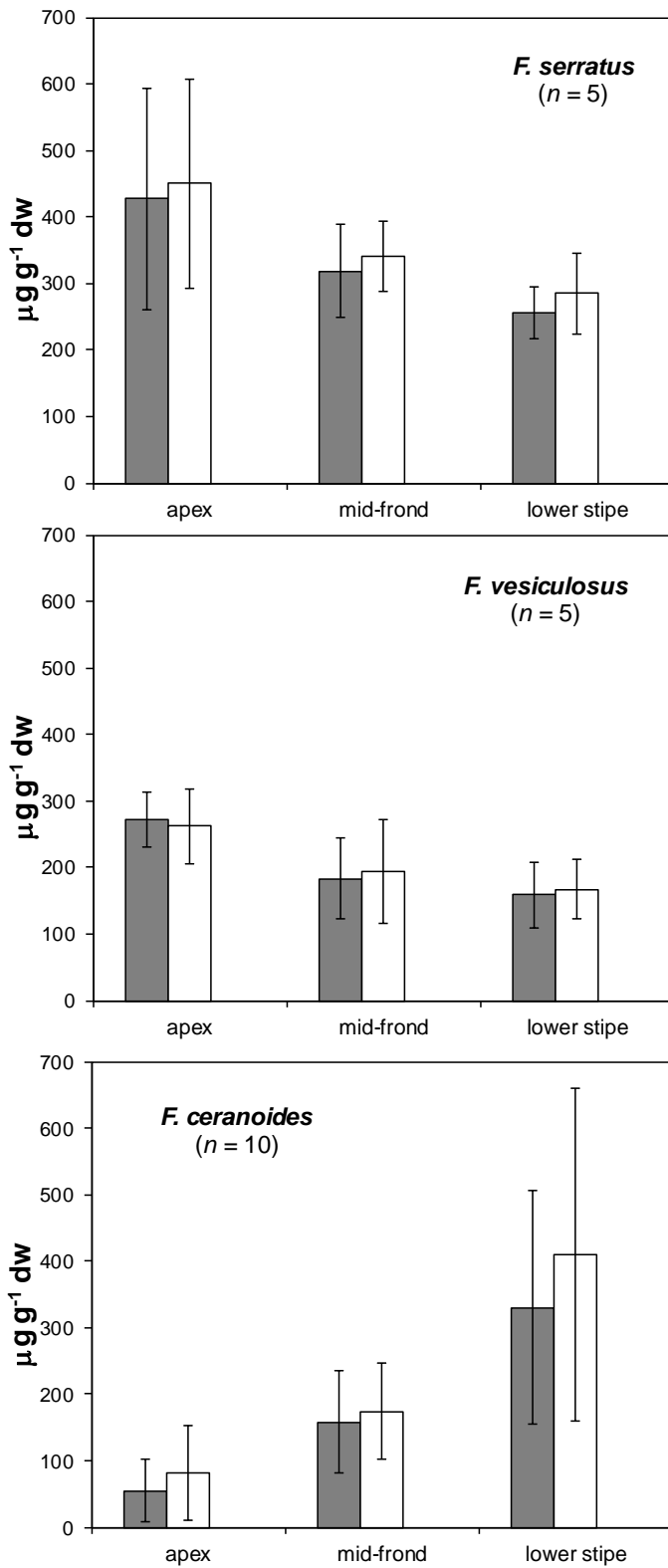
330

331 Figure 3: Dry weight concentrations of As in the different parts of the furoid species and as  
 332 returned by FP-XRF analysis of fresh sections (grey bars) and dry sections (open bars) and  
 333 by ICP-MS analysis following acid digestion (hatched bars). Errors represent the standard  
 334 deviation about the mean of  $n$  measurements.

335







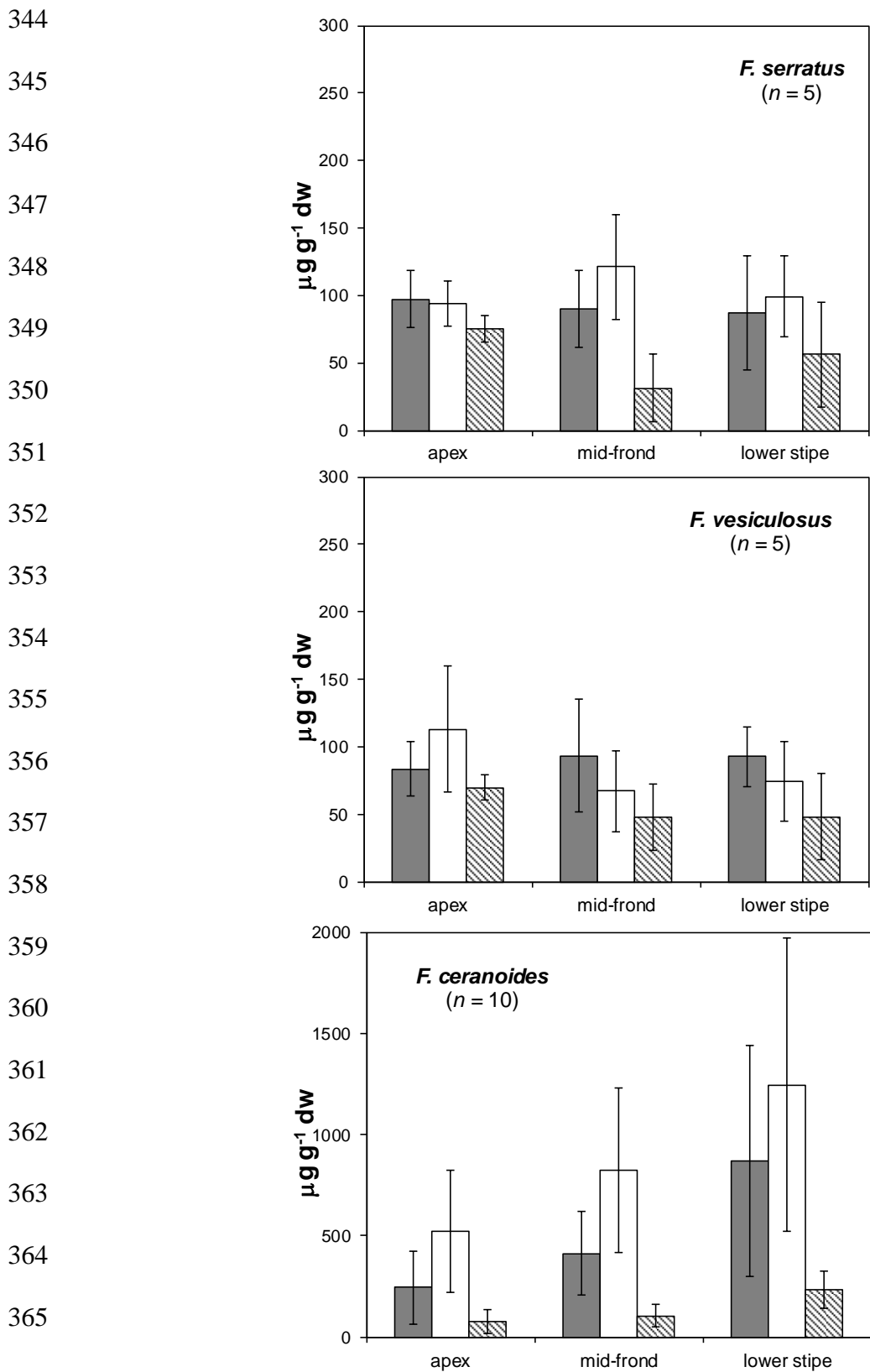
336

337 Figure 4: Dry weight concentrations of Br in the different parts of the fucoid species and as

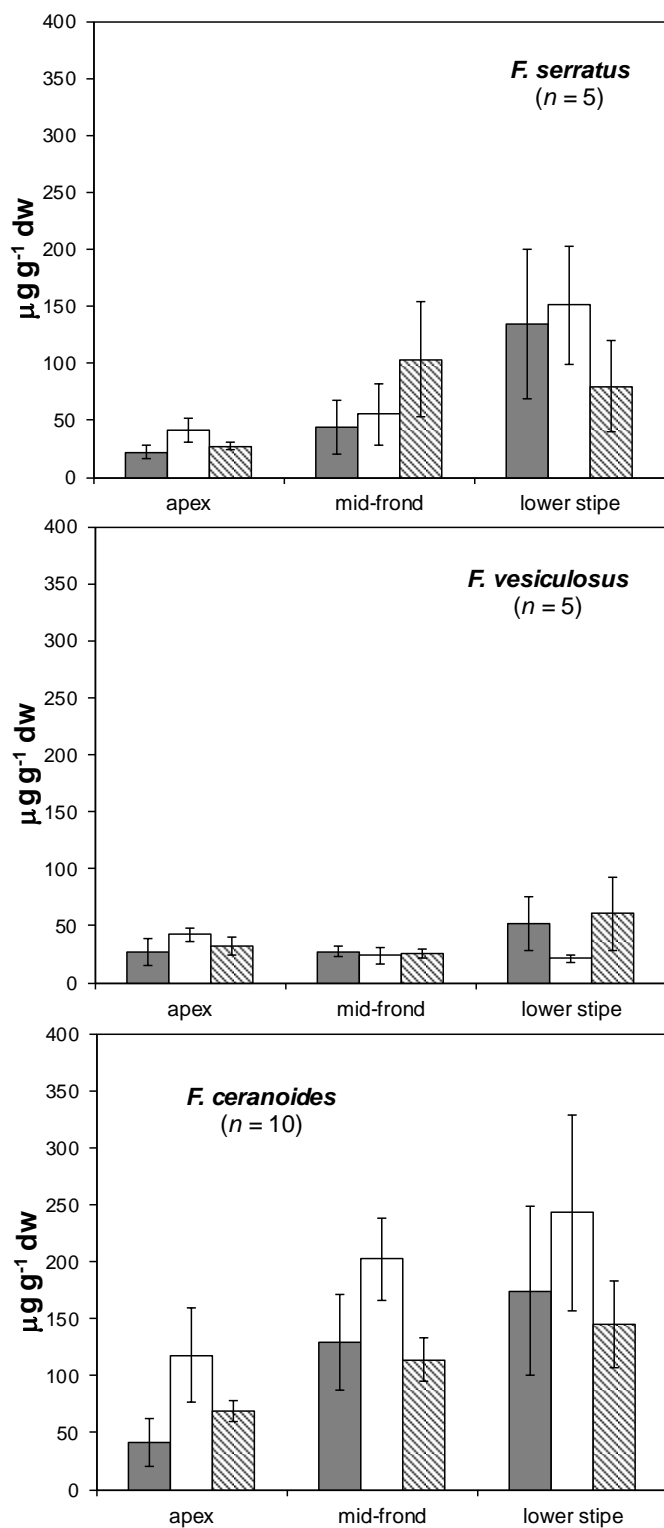
338 returned by FP-XRF analysis of fresh sections (grey bars) and dry sections (open bars).

339 Errors represent the standard deviation about the mean of *n* measurements.

340 Figure 5: Dry weight concentrations of Fe in the different parts of the furoid species and as  
 341 returned by FP-XRF analysis of fresh sections (grey bars) and dry sections (open bars) and  
 342 by ICP-MS analysis following acid digestion (hatched bars). Errors represent the standard  
 343 deviation about the mean of  $n$  measurements.



366 Figure 6: Dry weight concentrations of Zn in the different parts of the furoid species and as  
 367 returned by FP-XRF analysis of fresh sections (grey bars) and dry sections (open bars) and  
 368 by ICP-MS analysis following acid digestion (hatched bars). Errors represent the standard  
 369 deviation about the mean of  $n$  measurements.



371 *3.5. Summary and implications of findings*

372 In a previous article, we demonstrated the potential of FP-XRF for determining trace element  
373 concentrations in different species of dried coastal macroalgae in a laboratory accessory  
374 stand (Bull et al., 2017). The technique has distinct advantages over conventional methods  
375 involving sample digestion that include reduced time and costs, non-destruction of material  
376 (of particular significance to archived specimen banks), increased sample throughput,  
377 minimal operator training, capability of exploring tissue spatial variability and avoidance of  
378 hazardous wastes. Because monitoring in situ requires direct analysis without drying,  
379 however, the present study evaluated the effects of the presence of internal and surficial  
380 water on elemental concentrations returned for various fucoids. Thus, a comparison of  
381 results arising from the analysis of fresh sections that had been dry-weight normalised and  
382 the analysis of sections that had been subsequently freeze-dried revealed a greater sensitivity  
383 of the latter approach but results that were highly correlated for all elements considered.  
384 Lower dry-weight concentrations returned when analysed fresh are attributed to the  
385 absorption of characteristic x-rays by water contained within or at the surface of the  
386 macroalga.

387

388 Since variations in the percentage water in a given section of fucoid were small, with  
389 relative standard deviations of less than 5% in most cases, instantaneous, quantitative  
390 correction for macroalgal water content may be readily accomplished through species- and  
391 section-specific algorithms; alternatively, it is possible that the fluorescence of Cl ( $K_{\alpha} = 2.62$   
392 keV,  $K_{\beta} = 2.82$  keV) could be used as a direct proxy for water content if local salinity is  
393 known (Tjallingii et al., 2007). Additional, element-specific corrections for x-ray absorption  
394 by water based on the gradients of the relationships between samples analysed fresh and dry  
395 (Figure 2) would also be required for complete quantification of concentrations on a dry  
396 weight basis. In practice, corrections for the effects of water may be stored in the Niton XRF

397 software as alternative calibrations in the low density mode by adding appropriate slopes  
398 and, if necessary, intercepts.

399

400 In most cases, dry-weight concentrations of As and Zn obtained by the analysis of fresh and  
401 dried sections of fucoids by FP-XRF were not statistically different to corresponding  
402 concentrations derived independently by ICP-MS following acid digestion. For Fe in the  
403 estuarine macroalga, *F. ceranoides*, however, we attribute significantly lower results arising  
404 from ICP analysis to the incomplete release of Fe from the macroalga and to the presence of  
405 silt particles on the tissue surface that evaded cleaning and that were detected by the XRF  
406 but not completely digested by HNO<sub>3</sub>. Among the elements analysed, the latter effect would  
407 be most significant for Fe given its high concentration in fine sediment from the Tavy  
408 Estuary (about 60,000 µg g<sup>-1</sup> determined on dried, intertidal silt by FP-XRF in a higher  
409 density, ‘mining’ mode, and compared with As and Zn concentrations of 90 and 250 µg g<sup>-1</sup>,  
410 respectively). The heterogeneous dispersion of silt on the tissue surface would also account  
411 for the relatively high variability of Fe concentrations measured by XRF among replicates of  
412 the same sample section.

413

#### 414 3.4. Deployment of the XRF in situ

415 With the effects of macroalgal water evaluated and quantified, the feasibility of employing  
416 the Niton FP-XRF spectrometer in situ was tested. Thus, the Tavy Estuary was revisited and  
417 sections from *F. ceranoides* and *F. vesiculosus* analysed under the operating conditions  
418 described above (instrument mode, counting time, energy ranges) after cleaning in MQW,  
419 dissection, blotting dry and thickness measurement with callipers. Initial attempts using the  
420 XRF handheld against sections placed on a solid but smooth surface (e.g. a plastic tray on a  
421 flat rock) and activated manually via the tilting touchscreen proved unsuccessful for a  
422 number of reasons. For example, positioning the XRF window such that it covered the

423 macroalgal section completely was difficult, despite the aid of live video-footage generated  
424 by a colour charge-coupled device camera and sampling imaging system adjacent to the  
425 detector; moreover, once positioning had been accomplished, holding the instrument still for  
426 a suitable length of time against the slimy, fucoid surface was not possible. A moving x-ray  
427 source over a low density, irregular sample also poses a safety hazard to the operator through  
428 radiation scattering; although this hazard could be minimised by using a backscatter collar-  
429 shield around the nose of the instrument (Figure 7a), the additional size and weight of  
430 equipment further inhibited accurate and steady positioning of the detector window.

431

432 Successful application of the XRF in the field was, however, accomplished when coupled to  
433 a lightweight (~ 2.5 kg) and small-volume (300 cm<sup>3</sup>) mobile test-stand (ThermoScientific,  
434 PN 430-032) and laptop (Figure 7b). Here, the test-stand was placed on a level, stable  
435 surface and the instrument subsequently securely fixed to the steel baseplate with the nose  
436 pointing upwards. Individual sample sections were placed on polyester film and positioned  
437 centrally over the detector window with the aid of plastic tweezers and, if necessary, held  
438 flat and in place with weights (e.g. small stones) at each end (Figure 7c). Once the shielded  
439 (tungsten-plastic) stand lid was closed, measurements were activated remotely using the  
440 laptop and via USB.

441

442 Essentially, this is the same approach as that employed in the laboratory using the accessory-  
443 stand. Additional benefits of performing measurements in situ, however, include the  
444 development of a strategy or focus that is iterative or directly informed by immediate results,  
445 identification of contamination hot-spots, elements of concern or the effects of a pollution  
446 incident, determination of which samples to return to the laboratory for further  
447 characterisation, and little or no degradation of macroalgae should transport to the laboratory  
448 be otherwise time-consuming. With three people in the field and working concurrently on

449 separate tasks (sampling, sample processing and analysis), algal section throughput for a 200  
450 second counting time was about 15 per hour, and with a single, fully-charged battery, the  
451 XRF could be deployed for a period of up to six hours. Given the weight of equipment  
452 involved (about 15 kg for the XRF, stand, laptop and cases), set up and measurement are  
453 also possible with a single operator, although throughput would be significantly reduced  
454 because of the requirement for an individual to conduct multiple tasks successively or  
455 concurrently.

456

457 For different sections analysed in situ, concentrations measured directly were converted to  
458 dry weight concentrations using the average (generic) percentage water for a given type of  
459 section of a particular species and subsequently corrected for x-ray water absorption by  
460 applying the element-specific gradients defining the relationship between samples analysed  
461 fresh and dry (Figure 2). In Figure 8, results for As and Zn derived accordingly, [XRF-*in*  
462 *situ*], are shown for samples in which concentrations were subsequently determined by ICP-  
463 MS following drying and acid digestion. For both elements, correlations were significant ( $p$   
464  $< 0.05$ ) with  $r$  values exceeding the US EPA quantitative screening criterion of 0.7  
465 (Environmental Protection Agency, 2007). For Fe, concentrations derived in situ were  
466 significantly correlated with but considerably higher than those derived independently by  
467 ICP-MS for reasons outlined above. With respect to *F. vesiculosus* in the Tavy, mean  
468 concentrations of As and Zn derived in situ (67 and 200  $\mu\text{g g}^{-1}$ ) are also similar to mean  
469 values reported in the literature for the upper estuary (86 and 382  $\mu\text{g g}^{-1}$  respectively;  
470 Rainbow et al., 2011).

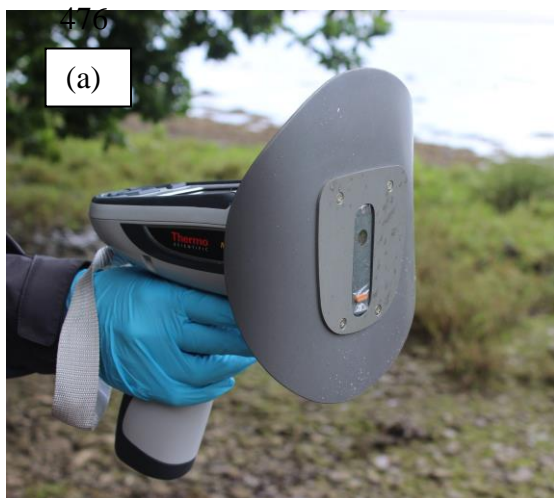
471

472

473

474

475



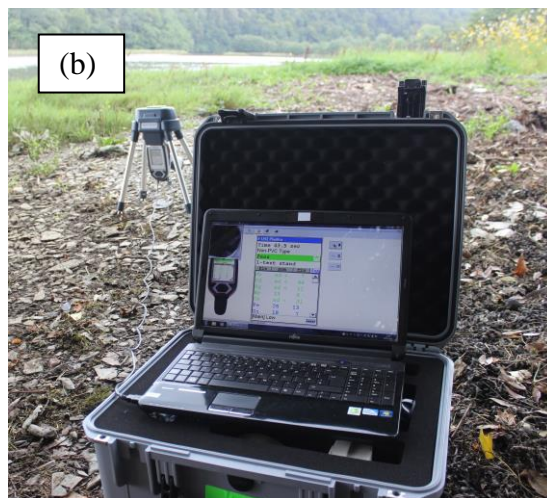
478

479

480

481

482



483

484

485

486

487

488

489

490

491



492 Figure 7: (a) The Niton XL3t plus backscatter shield; (b) configuration of the instrument in

493 situ and coupled to the portable stand and laptop; (c) a fucoid section placed above the

494 detector window and within the stand.

495

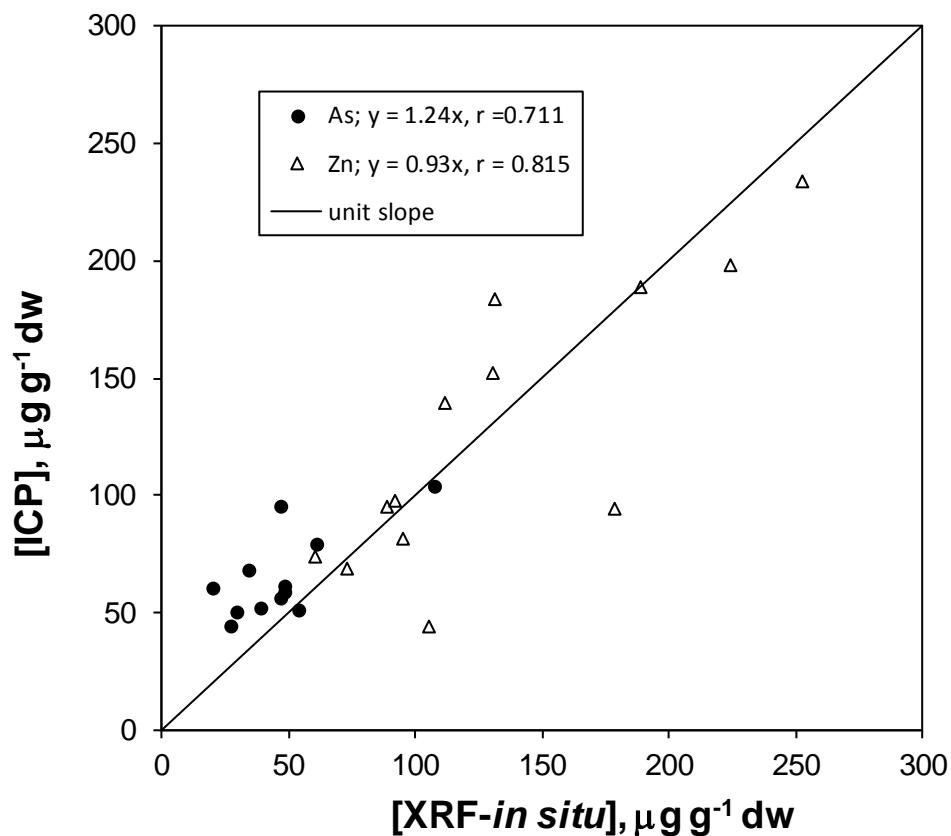
496

497

498



499 Figure 8: Relationship between As and Zn concentrations in *F. ceranoides* and *F.*  
 500 *vesiculosus* determined by ICP-MS following acid digestion and by FP-XRF deployed in  
 501 situ and after correction for the content and x-ray absorption of water.



#### 4. Conclusions

Although FP-XRF does not have the capability of sub-part per million analyses to replace atomic or mass spectrometry, this study has shown that the Niton XL3t provides a rapid, cost-effective and non-destructive means of measuring various trace elements in both fresh and dry fucoid species of macroalgae, provided that a low density mode with thickness correction is employed. The analytical conditions described (mode of application, collimation, counting time, energy ranges) allow the ready quantification of As to dry weight concentrations down to a few  $\mu\text{g g}^{-1}$  and Br, Fe and Zn to concentrations of a few tens of  $\mu\text{g g}^{-1}$ ; measurement of Cu and Pb in fucoids is also possible in moderately to highly contaminated sites. Coupled to a mobile test-stand and laptop, the instrument can be

525 deployed in situ for rapid diagnostic and strategic purposes and to evaluate intra- and inter-  
526 specific concentration variations, with full quantification possible after empirical adjustment  
527 of data for the effects of water on sample weight and x-ray absorption.

528

### 529 **Acknowledgements**

530 We are grateful to Dr Andrew Fisher for technical support during the ICP-MS analysis. This  
531 study was funded partly by a UoP HEIF V Marine Institute grant.

532

### 533 **References**

534 Brito, G.B., de Souza, T.L., Bressy, F.C., Moura, C.W.N., Korn, M.G.A., 2012. Levels and  
535 spatial distribution of trace elements in macroalgae species from the Todos os Santos Bay,  
536 Bahia, Brazil. *Marine Pollution Bulletin* 64, 2238-2244.

537

538 Boubonari, T., Malea, P., Kevrekidis, T., 2008. The green seaweed *Ulva rigida* as a  
539 bioindicator of metals (Zn, Cu, Pb and Cd) in a low-salinity coastal environment.  
540 *Botanica Marina* 51, 472-484.

541

542 Bruhn, A., Dahl, J., Nielsen, H.B., Nikolaisen, L., Rasmussen, M.B., Markager, S., Olesen,  
543 B., Arias, C., Jensen, P.D., 2011. Bioenergy potential of *Ulva lactuca*: Biomass yield,  
544 methane production and combustion. *Bioresource Technology* 102, 2595-2604.

545

546 Bull, A., Brown, M.T., Turner, A., 2017. Novel use of field-portable-XRF for the direct  
547 analysis of trace elements in marine macroalgae. *Environmental Pollution* 220, 228-233.

548

549 Cairrão, E., Pereira, M.J., Pastorinho, M.R., Morgado, F., Soares, A.M.V.M., Guilhermino,  
550 L., 2007. *Fucus* spp. as a mercury contamination bioindicator in costal areas (Northwestern  
551 Portugal). *Bulletin of Environmental Contamination and Toxicology* 79, 388-395.  
552

553 Chan, S.M., Wang, W.X., Ni, I.H., 2003. The uptake of Cd, Cr, and Zn by the macroalga  
554 *Enteromorpha crinita* and subsequent transfer to the marine herbivorous rabbitfish, *Siganus*  
555 *canaliculatus*. *Archives for Environmental Contamination and Toxicology* 44, 298-306.  
556

557 Di Narda, F., Toniolo, R., Bontempelli, G., 2001. Improved microwave digestion procedure  
558 for inductively coupled plasma mass spectrometric determinations of inorganic bromide  
559 residues in foodstuffs fumigated with methyl bromide. *Analytica Chimica Acta* 436, 245-  
560 252.  
561

562 Duarte, C.M., Losada, I.J., Hendricks, I.E., Mazarrasa, I., Marba, N., 2013. The role of  
563 coastal plant communities for climate change mitigation and adaptation. *Nature Climate*  
564 *Change* 3, 961-968.  
565

566 Environmental Protection Agency, 2007. Method 6200 - Field portable x-ray fluorescence  
567 spectrometry for the determination of elemental concentrations in soil and sediment.  
568 <http://www3.epa.gov/epawaste/hazard/testmethods/sw846/pdfs/6200.pdf>. Accessed 7/16.  
569

570 Guinda, X., Juanes, J.A., Puente, A., Revilla, J.A., 2008. Comparison of two methods for  
571 quality assessment of macroalgae assemblages, under different pollution types. *Ecological*  
572 *Indicators* 8, 743-753.  
573

574 Martin, M.H., Nickless, G., Stenner, R.D., 1997. Concentrations of cadmium, copper, lead,  
575 nickel and zinc in the alga *Fucus serratus* in the Severn estuary from 1971 to 1995.  
576 Chemosphere 43, 25–334.  
577

578 Matias, M.G., Arenas, F., Rubal, M., Pinto, I.S., 2015. Macroalgal composition determines  
579 the structure of benthic assemblages colonizing fragmented habitats. PLOS ONE 10, article  
580 e0142289, DOI: 10.1371/journal.pone.0142289.  
581

582 Mulholland, R., Turner, A., 2011. Accumulation of platinum group elements by the marine  
583 gastropod *Littorina littorea*. Environmental Pollution 159, 977-982.  
584

585 Parsons, C., Grabulosa, E.M., Pili, E., Floor, G.H., Roman-Ross, G., Charlet, L., 2013.  
586 Quantification of trace arsenic in soils by field-portable x-ray fluorescence spectrometry:  
587 Considerations for sample preparation and measurement conditions. Journal of Hazardous  
588 Materials 262, 1213-1222.  
589

590 Rainbow, P.S., 2006. Biomonitoring of trace metals in estuarine and marine environments.  
591 Australasian Journal of Ecotoxicology 12, 107-122.  
592

593 Rainbow, P.S., Kriefman, S., Smith, B.D., Luoma, S.N., 2011. Have the bioavailabilities of  
594 trace metals to a suite of biomonitors changed over three decades in SW England estuaries  
595 historically affected by mining? Science of the Total Environment 409, 1589-1602.  
596

597 Reis, P.A., Cassiano, J., Veiga, P., Rubal, M., Sousa-Pinto, I., 2014. *Fucus spiralis* as  
598 monitoring tool of metal contamination in the northwest coast of Portugal under the

599 European Water Framework Directives. Environmental Monitoring and Assessment 186,  
600 5447-5460.  
601  
602 Rüdél, H., Fliedner, A., Kosters, J., Schroter-Kermani, C ., 2010. Twenty years of elemental  
603 analysis of marine biota within the German Environmental Specimen Bank-a thorough look  
604 at the data. Environmental Science and Pollution Research 17, 1025-1034.  
605  
606 Sondergaard, J., Bach, L., Gustavson, K., 2014. Measuring bioavailable metals using  
607 diffusive gradients in thin films (DGT) and transplanted seaweed (*Fucus vesiculosus*), blue  
608 mussels (*Mytilus edulis*) and sea snails (*Littorina saxatilis*) suspended from monitoring  
609 buoys near a former lead-zinc mine in West Greenland. Marine Pollution Bulletin 78, 102-  
610 109.  
611  
612 Tabarsa, M., Rezaei, M., Ramezanpour, Z., Waaland, J.R., 2012. Chemical compositions of  
613 the marine algae *Gracilaria salicornia* (Rhodophyta) and *Ulva lactuca* (Chlorophyta) as a  
614 potential food source. Journal of the Science of Food and Agriculture 92, 2500-2506.  
615  
616 Tjallingii, R., Röhl, U., Kölling, M., Bickert, T., 2007. Influence of the water content on x-  
617 ray fluorescence core-scanning measurements in soft marine sediments. Geochemistry,  
618 Geophysics, Geosystems 8, Q02004, doi:10.1029/2006GC001393.  
619  
620 Turner, A., Solman, K.R., 2016. Analysis of the elemental composition of marine litter  
621 by field-portable-XRF. Talanta 159, 262-271.  
622

- 623 Viana, I.G., Aboal, J.R., Fernàndez, J.A., Real, C., Villares, R., Carballeira, A., 2010. Use of  
624 macroalgae stored in an Environmental Specimen Bank for application of some European  
625 Framework Directives. *Water Research* 44, 1713–1724.  
626
- 627 Zbikowski, R., Szefer, P., Latala, A., 2006. Distribution and relationships between selected  
628 chemical elements in green alga *Enteromorpha* sp from the southern Baltic. *Environmental*  
629 *Pollution* 143, 435-448.